aquaculture journal

MDPI

Article

Antifungal Activity and Protective Effects of Cetylpyridinium Chloride Against "Milky Disease" in Chinese Mitten Crab (*Eriocheir sinensis*)

Xuetong Wang [1,2], Yu Zhang [1,2], Changbo Zhou [1,2], Jiaxuan Wu [1,2], Chunyu Zhu [1,2] and Fangliang Zheng [1,2,*]

[1] College of Life Sciences, Liaoning University (Chongshan Campus), Shenyang 110036, China; wangxuetongv@163.com (X.W.); zhangyu20001012@gmail.com (Y.Z.); zhouchangbo@proton.me (C.Z.); 18643087057@163.com (J.W.); zhuchunyu@lnu.edu.cn (C.Z.)

[2] Microbial Resources Development and Utilization Research Laboratory of Liaoning University, Shenyang 110036, China

* Correspondence: flzheng1980@163.com

Abstract

The milky disease caused by *Metschnikowia bicuspidata* has severely affected the farming of Chinese mitten crabs (*Eriocheir sinensis*), yet there are still no effective and environmentally friendly control measures available. This study employed a drug-repositioning strategy, combined with virtual screening, in vitro antifungal tests, and in vivo experiments, to evaluate the effect of cetylpyridinium chloride (CPC) on the pathogen. Sterol 14α-demethylase (CYP51), the key enzyme in the ergosterol biosynthetic pathway, was selected as the candidate target for molecular docking. The docking results showed that CPC had a strong binding affinity (score −9 kcal/mol) to the predicted CYP51 active site, but its use as a direct target still requires further biochemical verification. In the in vitro experiment, CPC exhibited potent antifungal activity (MIC = 1.56 μg/mL, MFC = 3.125 μg/mL) and significantly reduced the formation of biofilms at the tested concentrations ($p < 0.05$). After feeding at a dose of 800 μg/g feed for 7 days, the activities of immune-related enzymes (ACP, AKP, LZM) and antioxidant enzymes (CAT, SOD, GPX) in the hepatopancreas of crabs significantly increased ($p < 0.05$), and no oxidative stress was induced. In the challenge test, the original cumulative mortality rate of group C (challenge + 800 μg/g CPC bait) was 59.72%, lower than that of group B (challenge + basal feed) at 75.00% (absolute risk reduction of 15.28 percentage points). The corrected survival rates were 40.0% (group C) and 24.4% (group B), but the group differences after correction by the generalized linear mixed model did not reach a statistically significant level ($p = 0.068$). The histopathological score showed that CPC significantly alleviated the severity of lesions in the hepatopancreas, gills, muscles, and heart ($p < 0.001$). Although the targeting mechanism of CPC against CYP51 requires further experimental validation, our findings suggest that CPC holds promise as a drug-repositioning candidate for managing milky disease in *E. sinensis*, particularly by boosting host immunity and mitigating tissue damage.

Keywords: *Eriocheir sinensis*; *Metschnikowia bicuspidata*; milky disease; cetylpyridinium chloride (CPC); antifungal activity

Academic Editors: Mirza Masum Beg and Yari Vecchio

Received: 25 July 2026
Revised: 30 August 2026
Accepted: 3 September 2026
Published: 18 September 2026

1. Introduction

The Chinese mitten crab (*Eriocheir sinensis*) is an important freshwater aquaculture species in China, renowned for its delicious meat and high nutritional value. Its edible

tissues are rich in high-quality protein, unsaturated fatty acids, and essential minerals [1]. In 2020, the national aquaculture production of *E. sinensis* reached 775,000 tons, with an output value exceeding 1.456 billion US dollars, forming a large-scale industrial cluster in provinces such as Jiangsu and Liaoning. By 2023, the production increased to 888,629 tons [2]. For instance, the production in Panjin City, Liaoning Province, was 60,000 tons in 2022 and 80,000 tons in 2024. The local river crabs were rated as high-quality agricultural products in China and have become an important pillar industry of the regional economy.

However, in recent years, the milky disease caused by *Metschnikowia bicuspidata* has severely affected this industry [3]. This disease is characterized by milky white exudate in the cephalothorax, liquefaction of the hepatopancreas, and lesions in the gills, with a mortality rate exceeding 75% [4,5]. The pathogen can spread rapidly through contaminated water bodies, feed, and seedlings, and repeatedly break out in major production areas such as Jiangsu and Liaoning, causing huge economic losses [6].

Currently, the prevention and control of milky disease mainly rely on disinfectants and fluconazole and other conventional antifungal drugs. However, long-term or improper use of these drugs can easily induce drug resistance, drug residues in aquatic products, and the disruption of microbial community structure in the breeding environment [7]. Most existing antifungal agents exert primarily direct fungicidal activity, yet they lack the capacity to enhance the host's physiological resistance and immune responses [8]. Therefore, the development of novel antifungal therapeutics with enhanced potential to ensure sustainable prevention and control of milky disease in Chinese mitten crabs has become an urgent priority [9].

Sterol 14α-demethylase (CYP51) is a member of the cytochrome P450 superfamily and a key enzyme in the fungal ergosterol biosynthesis pathway, which is crucial for maintaining the integrity of fungal cell membranes [10]. Inhibiting CYP51 can block ergosterol synthesis, leading to the accumulation of toxic sterol intermediates, and ultimately causing the inactivation of fungal cells. Due to its key function and significant structural differences from homologous proteins in mammals, CYP51 has become a classic and important antifungal drug target [11].

With the rapid development of artificial intelligence, structural biology, and high-performance computing, computer-aided drug design (CADD) has become an important tool for accelerating drug development. Among them, molecular docking can predict the interaction between small molecules and target proteins at the atomic level, conduct virtual screening of compound libraries, efficiently discover potential lead compounds, and reduce experimental costs [12]. Compared with drug repositioning (re-exploring the new indications of existing drugs), drug repositioning has the advantages of low development risk, low cost, and short cycle, and the related pharmacological and safety data are relatively complete [13].

In this study, CYP51, the key enzyme in ergosterol synthesis in *M. bicuspidata*, was selected as the molecular target [10]. Based on the compound library approved by the US Food and Drug Administration (FDA) in the ZINC database, a virtual screening based on molecular docking was conducted. The results showed that cetylpyridinium chloride (CPC) had excellent binding affinity with CYP51 and, thus, was selected as a candidate compound for in vitro and in vivo evaluation.

CPC is a quaternary ammonium salt compound widely used in oral care products [14]. It has excellent antibacterial activity, can inhibit various bacteria and fungi, and has good safety and tolerance [15,16]. However, there are few reports on its antifungal activity against *M. bicuspidata* and its mechanism of action.

The aim of this study is (1) to analyze the interaction between CPC and *M. bicuspidata* CYP51 through molecular docking; (2) to evaluate the in vitro antifungal activity and biofilm inhibition ability of CPC; and (3) to explore its safety, antioxidant effect, and in vivo therapeutic effect on *E. sinensis*.

This study explores the application potential of the quaternary ammonium salt compound cetylpyridinium chloride as an antifungal candidate drug in the prevention and control of crustacean aquaculture diseases.

2. Materials and Methods

2.1. Fungal Strain and Culture Conditions

The *M. bicuspidata* strain used in this study was provided and preserved by the Pathogenic Fungi Research Center of Liaoning University. The strain was first cultured on a Modified Bengal Red solid medium at 28 °C for 48 h to obtain a single colony with typical morphology and stable growth status. Then, the single colony was inoculated into a YPD (yeast extract peptone glucose) liquid medium and cultured at 28 °C, 180 r/min in an orbital shaker until the logarithmic growth phase. The fungal cell concentration was counted using a hemocytometer and corrected by the streaking method. Finally, the fungal suspension was adjusted to the required concentration for the experiment.

2.2. Virtual Screening of Small-Molecule Drugs Targeting the CYP51 Protein

Virtual screening was performed targeting lanosterol 14α-demethylase (CYP51), a key enzyme in ergosterol biosynthesis. The amino acid sequence of CYP51 from *M. bicuspidata* (UniProt accession: A0A4P9ZFU2) was retrieved from the UniProt database. Its three-dimensional structure was predicted using the RoseTTAFold module on the Robetta server. Model quality was assessed using the SAVES v6.0 platform, incorporating PROCHECK, a Ramachandran plot analysis, VERIFY3D, and ERRAT. The model with the highest overall quality score was selected for subsequent active-site prediction and molecular docking.

The active pocket was predicted using the DoGSiteScorer algorithm, and key active regions were defined based on reported binding characteristics of CYP51 inhibitors. Prior to docking, protein preparation—including dehydration, hydrogenation, and charge assignment—was performed using AutoDock Tools-1.5.7, and the grid box coordinates were determined. High-throughput molecular docking was carried out using AutoDock Vina, with each docking run independently repeated 20 times. Candidate small molecules were initially selected based on binding free energy, spatial complementarity, and interaction modes. Finally, the protein–ligand complexes were visualized with PyMOL-3.1 to elucidate the key binding sites and interaction patterns [17].

2.3. Evaluation of In Vitro Antifungal Activity

2.3.1. Drug Susceptibility Test

The drug susceptibility test was conducted according to the CLSI M27-A3 yeast standard protocol, with appropriate adjustments. All drugs were prepared as working solutions using YPD liquid medium. Logarithmic growth phase yeast cells were collected, centrifuged, and resuspended in YPD medium; the final inoculation concentration of the fungal suspension was adjusted to 1×10^5 CFU/mL by using a hemocytometer combined with OD60Onm calibration.

Disk diffusion assay: Sterile filter paper discs were immersed in 10 μg/mL CPC solution and placed on a Rose Bengal Agar medium plate pre-coated with yeast cell suspension. Three biological replicates were set. After culturing at 28 °C for 48 h, the diameter of the inhibition zone was measured.

Determination of MIC and MFC: The minimum inhibitory concentration (MIC) and minimum fungicidal concentration (MFC) of cetylpyridinium chloride (CPC) against the test yeast strain were determined using the broth microdilution method in 96-well flat-bottom plates. A CPC stock solution (100 μg/mL) was serially twofold-diluted in YPD broth and then mixed with an equal volume of yeast inoculum, yielding final CPC concentrations ranging from 50 to 0.098 μg/mL (twofold dilution series). The final yeast cell density was adjusted to approximately 1×10^5 CFU/mL. Each plate included a positive growth control (yeast suspension without CPC) and a negative sterility control (sterile YPD medium without yeast and drug). After incubation at 28 °C for 72 h, the optical density at 600 nm (OD_{600}) was measured using a ReadMax 1200 absorbance microplate reader (Shanghai Flash Spectrum Biological Technology Co., Ltd., Shanghai, China). The MIC was defined as the lowest CPC concentration that inhibited ≥80% of yeast growth relative to the positive control, as calculated from the OD_{600} values.

For MFC determination, 100-μL aliquots were taken from wells showing no visible growth (i.e., those with OD_{600} below the MIC threshold, corresponding to concentrations at or above the MIC) and spread onto fresh Rose Bengal agar plates. These plates were incubated at 28 °C for 48 h, and the MFC was recorded as the lowest CPC concentration that yielded ≤ 5 fungal colonies per spot. The positive growth control on agar plates exhibited confluent growth, confirming the viability and validity of the assay. Three replicate wells were tested for each concentration, and the entire experiment was independently repeated three times.

2.3.2. Biofilm Inhibition Assay

The inhibitory effect of CPC on yeast biofilm formation was evaluated using the crystal violet staining method [18]. A yeast suspension was prepared at a density of 1 × 107 CFU/mL in YPD medium. CPC was serially twofold diluted starting from 12.5 μg/mL and then mixed with an equal volume of the yeast suspension in 96-well flat-bottom plates, yielding final CPC concentrations ranging from 6.25 to 0.098 μg/mL (twofold dilution series). The plates were incubated at 28 °C for different time intervals (3, 12, 24, and 48 h) to assess the time-dependent effect, with separate parallel plates prepared for each time point.

For each time point, the following controls were included: (i) a growth control (yeast suspension with the same volume of solvent but without CPC), (ii) a medium blank (sterile YPD medium only), and (iii) a solvent control (YPD medium with solvent but without yeast) to verify that the solvent itself did not interfere with the assay. The solvent control consistently showed absorbance values comparable to the medium blank, confirming the absence of solvent interference. Each concentration and control was tested in triplicate wells.

After incubation, the culture medium was gently discarded, and the wells were rinsed twice with distilled water to remove non-adherent yeast cells. The attached biofilms were fixed and stained with 200 μL of 0.4% (w/v) crystal violet solution for 15 min at room temperature. The wells were then thoroughly washed with distilled water to remove excess stain, and the crystal violet retained by the biofilms was solubilized with 200 μL of 95% ethanol. The absorbance of each well was measured at 590 nm using a microplate reader. The biofilm inhibition rate was calculated according to the following formula:

$$\text{Biofilm inhibition rate (\%)} = [1 - (OD_{590,\text{ treatment}} - OD_{590,\text{ mean plank}})/(OD_{590,\text{ growth}} - OD_{590,\text{ mean plank}})] \times 100\%$$

where $OD_{590,\ treatment}$ is the absorbance of the CPC-treated well, $OD_{590,\ growth}$ is the absorbance of the growth control (yeast without CPC), and $OD_{590,\ mean\ plank}$ is the absorbance of the medium blank.

2.4. Animal Experimental Design and Administration Protocol

2.4.1. Experimental Animals and Grouping

Juvenile *E. sinensis* (weight 5.40 ± 0.26 g) were purchased from a crab seed breeding base in Nantong City, Jiangsu Province. Upon arrival, the crab seedlings were acclimated in plastic aquaria (8 L) pre-treated with disinfectant for 7 days, with a rearing density of 30 crabs per tank. The tanks were covered with netting to prevent escape. The tank openings were covered with mesh to prevent escape. During the acclimation period, the water temperature was maintained at the natural temperature, the base feed was fed twice a day, and the leftover food and dead individuals were promptly cleaned.

Before the formal experiment, 10 juvenile crabs were randomly selected, and PCR was used to confirm that they were free of *M. bicuspidata* infection. Only crabs with intact body shape and sensitive responses were included in the experiment. Healthy juvenile crabs were randomly divided into a CPC treatment group and a control group, with 3 replicates in each group and 30 crabs in each replicate. The CPC group was fed the medicated feed prepared at a dose of 800 μg/g for 7 consecutive days, after which they were switched to the basic feed. The control group was continuously fed the regular feed for the entire period, which was used for enzyme activity measurement.

Feeding and water quality management: During both the acclimation and formal experimental periods, feeding was performed once daily at 9:00. The daily feed ration was initially set at 5% of the crab's wet body weight, and the actual feeding amount was adjusted in real time based on daily feed consumption and crab mortality to avoid overfeeding and water deterioration. To maintain the stability of the aquaculture environment, approximately three-quarters of the water volume in each rearing basin was replaced daily by siphoning, accompanied by the prompt removal of feces, residual feed, and other metabolic wastes to ensure consistent water cleanliness.

Environmental conditions: During the acclimation period, the water temperature was maintained at 18 ± 1 °C. During the formal experiment, water quality parameters were controlled within the following ranges: dissolved oxygen > 6.0 mg/L, ammonia nitrogen < 0.2 mg/L, nitrite < 0.05 mg/L, water temperature 22 ± 1 °C, and pH 7.8–8.2. Dead crabs were checked and recorded daily at 08:00, and any dead individuals were immediately removed from the basins to prevent water contamination and disease transmission.

Dose selection rationale: The theoretical effective dose range was estimated by proportional scaling from the in vitro MIC (≈1.56 μg/mL) and oral bioavailability of CPC. Since 400 μg/g feed failed to significantly improve survival in preliminary trials, we raised the dose to 800 μg/g (still within the safety limit) as a qualitative screening test to verify whether oral CPC confers protective potential against *E. sinensis* milky disease.

2.4.2. Feed Preparation

The experimental diets were prepared according to the ingredient mass ratios specified in Tables 1 and 2. All raw materials were accurately weighed and thoroughly blended to obtain a homogeneous dry powder mixture. Distilled water was then gradually added to the mixed powders with continuous stirring until a uniform, viscous paste-like consistency was achieved. The resulting paste was steamed in an autoclave at 100 °C for 1 min to gelatinize the starch and condition the feed matrix. After cooling, the cooked material was transferred to a pelletizer and extruded into pellets approximately 3–5 mm in length. The

pellets were then air-dried in a cool, well-ventilated area until constant weight was reached, yielding the final dry experimental feed.

Table 1. CPC Insecticide Formula.

Ingredient	Content (%)
Corn flour	59.065
Bean meal	16.256
Protein by-product meal	16.256
Fish meal	5.419
Calcium dihydrogen phosphate	2.168
Sodium chloride	0.434
Vitamin premix	0.027
Choline	0.217
Ecdysterone	0.108
CPC	0.080

Table 2. Vitamin Premix Formula.

Ingredient	Content (%)
Vitamin A	6.59
Vitamin D	0.97
Vitamin E	24.39
Vitamin K	0.64
Vitamin B1	2.44
Vitamin B2	6.59
Vitamin B6	3.65
Pantothenic Acid	14.39
Nicotinic Acid	40.20
Biotin	0.14

For the preparation of medicated feeds, the required amount of CPC (calculated as the ratio of pure drug mass to basal diet mass) was first dissolved in the distilled water used for mixing, ensuring uniform drug incorporation throughout the feed matrix. All medicated feeds were prepared fresh prior to each feeding session. The basal diet formulation (without CPC) served as the control.

2.4.3. Sample Collection and Biochemical Index Determination

Hemolymph and hepatopancreas samples were collected on days 1, 3, 5, and 7 throughout CPC administration, and on day 14 of the experiment (7 days following cessation of CPC treatment). For hemolymph collection, the samples were centrifuged at 3000× *g* for 10 min at 4 °C to obtain serum, which was then stored at −80 °C until further analysis.

Serum biochemical parameters, including acid phosphatase (ACP), alkaline phosphatase (AKP), and lysozyme (LZM) activities, were determined using commercial assay kits (Beijing Boxbio Science & Technology Co., Ltd., Beijing, China) following the manufacturer's instructions patterns [19]. Hepatopancreas tissues were homogenized on ice, and the resulting supernatants were used to measure the activities of catalase (CAT), superoxide dismutase (SOD), total antioxidant capacity (T-AOC), and glutathione peroxidase (GPX), as well as the malondialdehyde (MDA) content, according to the protocols provided by the same manufacturer [20,21].

2.5. Challenge Protection Experiment and Pathological Observation

2.5.1. Challenge Model and Protection Experiment

The infection model was established using the immersion challenge method. A suspension of *M. bicuspidata* fungus was added to the aquaculture water, maintaining a final concentration of 1×10^7 CFU/mL, and the attack was carried out for 2 days. During this period, the water was completely replaced, and the fungal suspension was supplemented every day to ensure a constant concentration [22].

Firstly, the high-dose safety verification test included 2 treatment groups (each group had 3 replicates, and each replicate had 30 individuals): one group was fed 200 mg/g CPC feed, and the other group was fed the same amount of basic feed. The experimental period was 28 days. The primary endpoint was cumulative mortality; secondary endpoints included abnormal behavioral responses observed (e.g., lethargy, loss of righting reflex, or abnormal swimming) and gross pathological changes observed during necropsy. It should be noted that this safety trial was designed as a preliminary assessment of overt toxicity and mortality and did not include comprehensive evaluations such as histopathological examination of major organs, serum biochemical profiling, or drug residue analysis. However, due to the lack of detailed toxicological endpoints, a definitive conclusion regarding the complete safety profile of CPC cannot be drawn. Long-term or multi-dose safety studies with more comprehensive endpoints are warranted in future investigations.

Subsequently, the challenge treatment model included 3 treatment groups (each group had 3 replicates, and each replicate had 30 individuals): group A was the healthy control group (no challenge + basic feed, only for simulation operations), group B was the challenge control group (challenge + basic feed), and group C was the CPC treatment group (challenge + 800 μg/g CPC bait). The experimental period was 21 days. The breeding conditions were consistent with those in Section 2.4.1, and the number of dead individuals was recorded daily. The treatment effect of CPC on milky disease in *E. sinensis* was statistically analyzed.

Every day, observe and record the death situation. Immediately remove the dead crabs for dissection and record the incidence of milky liquidization lesions in the hepatopancreas. Aseptically collect the exudate from the hepatopancreas, streak it onto the Bengal Red plate, and incubate at 28 °C for 48 h to calculate the re-isolation rate of *M. bicuspidata* to confirm the cause of death concentration [23].

2.5.2. Histopathological Observation

At the end of the experiment, eight juvenile crabs were randomly selected from each group. They were anesthetized by ice-bath immersion for 5 min until the loss of righting reflex, and the body surface was then disinfected with 75% ethanol. Under sterile conditions in a laminar flow hood, an aseptic dissection was performed to collect hepatopancreas, muscle, heart, and gill tissues. All samples were immediately fixed in 4% paraformaldehyde solution.

The fixed tissues were sent to Liaoning Jijia Biotechnology Co., Ltd. (Shenyang, China) for histological processing. Standard hematoxylin–eosin (HE) staining was applied to prepare tissue sections. Systematic histopathological observation and comparative analysis were carried out on sections from all experimental and control groups to evaluate the effects of different treatments on tissue architecture [24,25].

Pathological alterations in each tissue were examined under a light microscope, with particular attention paid to the integrity of hepatopancreatic cellular structure and the distribution of fungal infection foci [21].

2.6. Statistical Analysis

All statistical analyses were performed using SPSS 23.0 (IBM Corp., Armonk, NY, USA) and R 4.2.1 (R Core Team, Vienna, Austria). Data were expressed as the mean ± standard error of the mean (SEM) or the mean ± standard deviation (SD), depending on the data distribution characteristics.

Two-group comparisons: The inhibition zone diameters from the disc diffusion test were compared between the CPC-treated group and the sterile water control group using the independent-samples *t*-test.

Multi-group comparisons: For comparisons among multiple treatment groups (e.g., biofilm inhibition rates at different CPC concentrations, tissue liquefaction rates in the challenge test, re-isolation rates of the pathogenic fungus, and cumulative mortality rates), one-way analysis of variance (ANOVA) was applied. When a significant overall difference was detected, Tukey's honest significant difference (HSD) was further conducted for post hoc pairwise comparisons, with significant differences denoted by different letters.

Repeated-measures data: Data collected at multiple time points (e.g., serum enzymatic activities, antioxidant enzyme activities, and time-course biofilm inhibition rates) were analyzed using repeated-measures ANOVA, with treatment group as the between-subjects factor, time as the within-subjects factor, and the group-by-time interaction term included in the model. When the sphericity assumption was violated, the Greenhouse–Geisser correction was applied.

Survival analysis (challenge protection test): Since the survival data were binomial in nature, involved repeated daily measurements, and included random effects from replicate rearing tanks, a generalized linear mixed model (GLMM) was employed. The model was fitted with a binomial error distribution and a logit link function. Treatment group (groups A, B, and C) was set as a fixed effect, while replicate tanks were included as a random effect (random intercept). Daily cumulative mortality counts were incorporated as a covariate to adjust for potential baseline differences in mortality among replicates. The model generated corrected marginal mean survival rates and their 95% confidence intervals (CIs) for each group. Pairwise comparisons of fixed effects were adjusted using the Tukey method, and odds ratios (ORs) with 95% CIs were calculated. All survival-related statistical inferences were based on this GLMM; raw mortality rates were used only for descriptive presentation.

Non-normally distributed data. Histopathological scores, which did not follow a normal distribution, were compared between groups using the Mann–Whitney U test and expressed as the median with interquartile range (IQR).

Significance levels and experimental replication. All tests were two-tailed, and the significance threshold was set at $\alpha = 0.05$. Significance levels are denoted as follows: $p < 0.05$ (significant), $p < 0.01$ and $p < 0.001$ (highly significant), and ns (not significant, $p \geq 0.05$). All in vitro experiments were performed with three independent biological replicates (each representing a separate experiment), while the in vivo challenge and safety tests were conducted using three replicate rearing tanks per treatment, with 30 crabs per tank. Data collection and analysis were performed independently for each replicate.

2.7. Ethical Statement

All operations involving *E. sinensis* in this study complied with the relevant ethical norms for the feeding and use of aquatic animals issued by the state and institutions.

3. Results

3.1. Molecular Docking and Screening Results

The three-dimensional structure of the CYP51 protein was predicted using the RoseTTAFold module of the Robetta server, and the highest-scoring model (result-1) was

selected for further analysis (Figure 1; Table 3). The protein sequence corresponding to the active-site region (α-helices 9–12) of result 1 was extracted using PyMOL (Figure 2) and submitted to DoGSiteScorer for active pocket prediction (Figure 3). Among the predicted pockets, pocket 1 exhibited the largest volume (1669.57 $Å^3$) and the highest drug score (0.81) and was, therefore, designated as the optimal docking region.

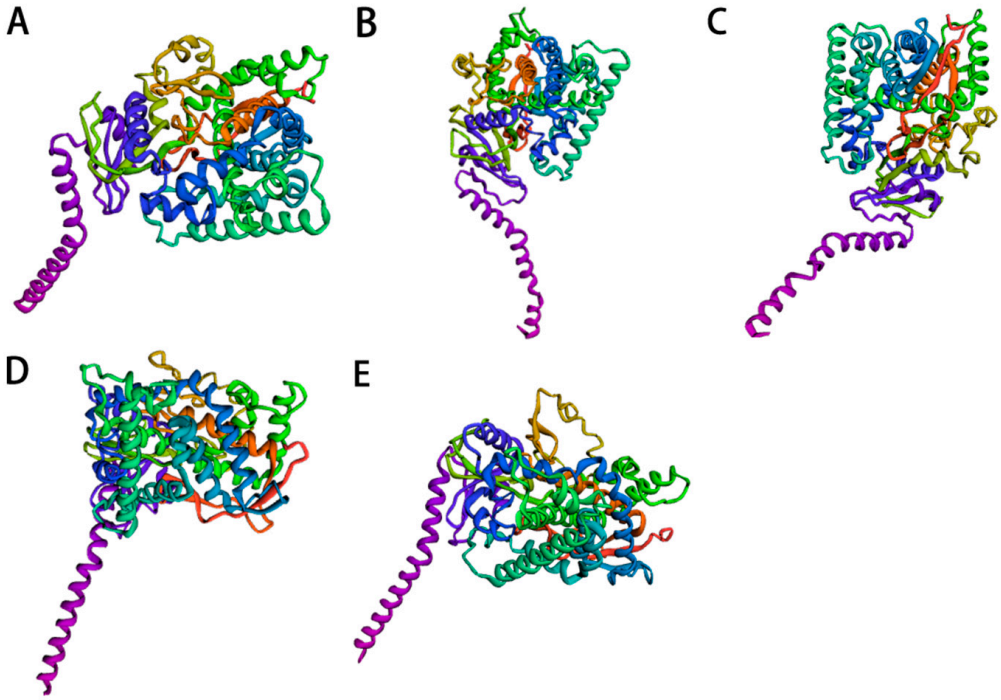

Figure 1. Robetta predicts the three-dimensional structure of the Sterol 14α-demethylase. (**A**) Model 1; (**B**) Model 2; (**C**) Model 3; (**D**) Model 4; (**E**) Model 5. Protein structures were visualized in PyMOL using default rainbow color scheme.

Table 3. Predicted binding pockets of CYP51.

Pocket Number	Volume ($Å^3$)	Surface ($Å^2$)	Drug Score	Simple Score
1	1669.57	2027.06	0.81	0.65
2	367.81	570.68	0.7	0.22
3	249.15	399.08	0.42	0.14

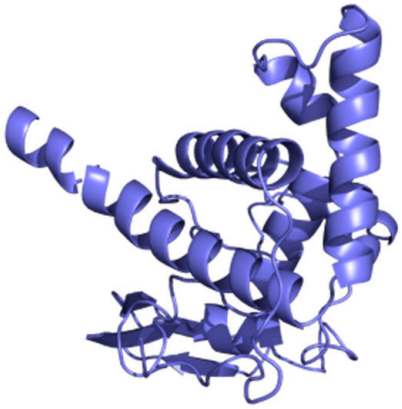

Figure 2. Three-dimensional structure of the active region.

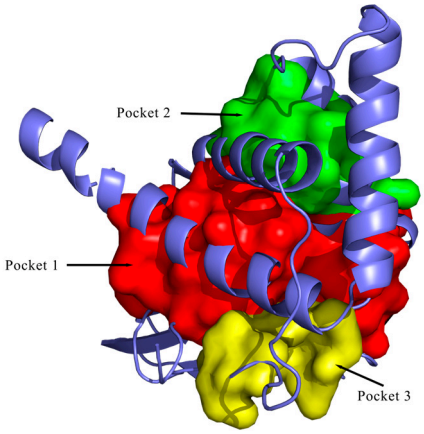

Figure 3. Combined prediction results of the pockets.

After pre-processing with AutoDock (Table 4), batch molecular docking was performed using AutoDock Vina against an FDA-approved small-molecule drug library. The binding energies of the successfully docked compounds were compared (Tables 5 and 6). The docking results revealed that CPC exhibited a binding energy of −9 kcal/mol to CYP51, which was comparable to those of clinical antifungal agents such as terbinafine and isavuconazole (Figure 4) [26].

Table 4. Dimensions and Coordinates of the Boxes.

Serial Number	Center_x	Center_y	Center_z	Size_x	Size_y	Size_z
1	−6.668	45.672	−65.554	38	30	34
2	1.474	51.227	−75.337	20	22	20

Table 5. Molecular-docking results of Box 1.

Serial Number	Generic Name	Molecular Formula	Binding Energy	Drug Efficacy
1	Methylergonovine	$C_{20}H_{25}N_3O_2$	−9	Vasopressor, for treating postpartum hemorrhage
2	Artemether	$C_{16}H_{26}O_5$	−9	Malaria parasite intracellular stage killing agent
3	Isavuconazonium	$C_{35}H_{35}F_2N_8O_5S^+$	−9	Used for treating fungal or yeast infections
4	Terbinafine	$C_{21}H_{25}N$	−9	Inhibit the synthesis of ergosterol in fungal cells
5	CPC	$C_{21}H_{38}N^+$	−9	Effective in killing various types of bacteria
6	Eflornithine	$C_6H_{12}F_2N_2O_2$	−8.9	Regulating cell division can kill trypanosomes
7	Rotigotine	$C_{19}H_{25}NOS$	−8.9	Regulating cell division can kill trypanosomes
8	Meloxicam	$C_{14}H_{13}N_3O_4S_2$	−8.9	It has anti-inflammatory, analgesic and antipyretic effects
9	Diazepam	$C_{16}H_{13}ClN_2O$	−8.9	Used for treating anxiety disorders and functional neuroses
10	Remifentanil	$C_{20}H_{28}N_2O_5$	−8.9	Used as an auxiliary anesthetic drug
11	Ambrisentan	$C_{22}H_{22}N_2O_4$	−8.8	Used for the treatment of pulmonary arterial hypertension
13	Cellcept	$C_{23}H_{31}NO_7$	−8.8	An immunosuppressant

Table 6. Molecular-docking results of Box 2.

Serial Number	Generic Name	Molecular Formula	Binding Energy	Drug Efficacy
1	Bcnu	$C_5H_9Cl_2N_3O_2$	−8.3	Tumor chemotherapy
2	Lopid	$C_{15}H_{22}O_3$	−8.2	Reduce cholesterol in the blood
3	Ihd	$C_6H_9NO_6$	−8	Ischemic heart disease Osteoporosis
4	Raloxifene	$C_{28}H_{27}NO_4S$	−8	Antidepressant
5	Tranylcypromine	$C_9H_{11}N$	−8	Cardiac adverse reactions
6	Frovatriptan	$C_{14}H_{17}N_3O$	−7.9	Treatment of asthma
7	Vilanterol	$C_{24}H_{33}Cl_2NO_5$	−7.9	Treatment of epilepsy
8	Klonopin	$C_{15}H_{10}ClN_3O_3$	−7.9	Sedative
9	Pentobarbital	$C_{11}H_{18}N_2O_3$	−7.9	As an eye drop to dilate the pupil
10	Hydroxyamphetamine	$C_9H_{13}NO$	−7.9	Tumor chemotherapy

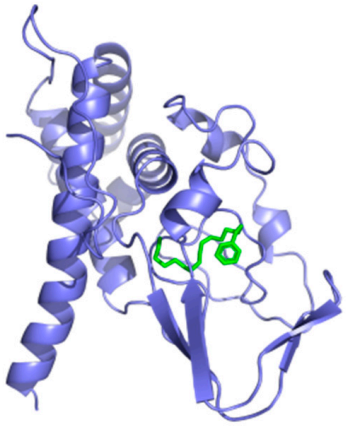

Figure 4. Molecular-docking results. Semi-flexible molecular docking between CPC (ligand, green) and the active pocket of lanosterol 14α-demethylase (receptor, blue).

Although several FDA-approved compounds showed docking binding energies around −9 kcal/mol, it should be noted that molecular-docking scores alone cannot serve as conclusive evidence for target inhibition or candidate drug selection. Therefore, we performed a multi-dimensional assessment that integrated in vitro antifungal activity (MIC/MFC), commercial availability, and aquaculture application costs. Based on this comprehensive evaluation, CPC was selected for subsequent in vitro and in vivo antifungal studies, showing potential as a candidate drug for the treatment of *M. bicuspidata* infections.

3.2. In Vitro Antifungal Activity

Following the identification of CPC as a candidate targeting CYP51 of *M. bicuspidata*, its in vitro antifungal activity was further evaluated by determining the inhibition zone diameter, minimum inhibitory concentration (MIC), and minimum fungicidal concentration (MFC). In the disc diffusion assay, CPC at 10 μg/mL produced an inhibition zone of 4.83 ± 1.26 mm in diameter (Figure 5; Table 7). The broth microdilution assay revealed that the MIC and MFC of CPC against *M. bicuspidata* were 1.56 μg/mL and 3.125 μg/mL, respectively (Table 8). Furthermore, CPC at 3.125 μg/mL (1× MFC) inhibited biofilm formation by 95.7%, with a significant inhibitory effect observable as early as 3 h post-incubation (Figures 6 and 7).

Figure 5. The inhibitory effect of CPC on *M. bicuspidata* (*n* = 3 replicates). A: Control (sterile water); B: Treatment with 10 mg/mL CPC.

Table 7. Measurement Results of Inhibition Zones (*n* = 3 replicates). * indicates significant difference ($p < 0.05$). Data were analyzed using an independent-samples *t*-test.

Name	Concentration (μg/mL)	Bacteriostatic Zone Diameter (mm)
Sterile water	—	—
CPC	10	4.83 ± 1.26 *

Table 8. The determination results of MIC and MFC of CPC for *E. sinensis* (*n* = 3 replicates).

Name	MIC (μg/mL)	MFC (μg/mL)
CPC	1.5625	3.125

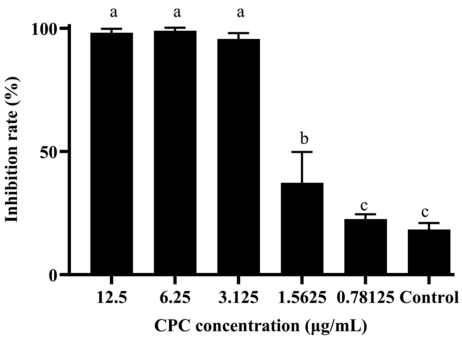

Figure 6. Measurement results of the biofilm. Values marked with different letters show significant differences ($p < 0.05$) (*n* = 3 replicates). a: groups treated with 12.5, 6.25 and 3.125 μg/mL CPC; no significant differences were observed among these groups. b: group treated with 1.5625 μg/mL CPC; significantly different from groups marked a and c. c: group treated with 0.78125 μg/mL CPC and the control group; no significant difference between these two groups, while they were significantly different from groups a and b.

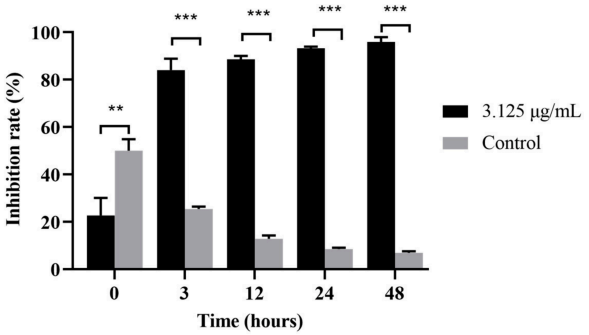

Figure 7. The determination results of the inhibition rate of the drug on the formation of biofilms at different stages (*n* = 3 replicates). Data are presented as mean ± standard error of the mean (SEM). The number of asterisks indicates different significant differences (** < 0.01, *** < 0.001).

3.3. Immune and Antioxidant Responses

Dietary supplementation with CPC at 800 μg/g significantly enhanced the activities of immune-related enzymes in the serum of *E. sinensis* (Figure 8). During the administration period (days 3–7), the activities of acid phosphatase (ACP) and alkaline phosphatase (AKP) in the CPC-treated group increased by 38.2% and 29.6%, respectively, relative to the control group. Lysozyme (LZM) activity reached its peak on day 5, showing a 45.3% increase over the control group.

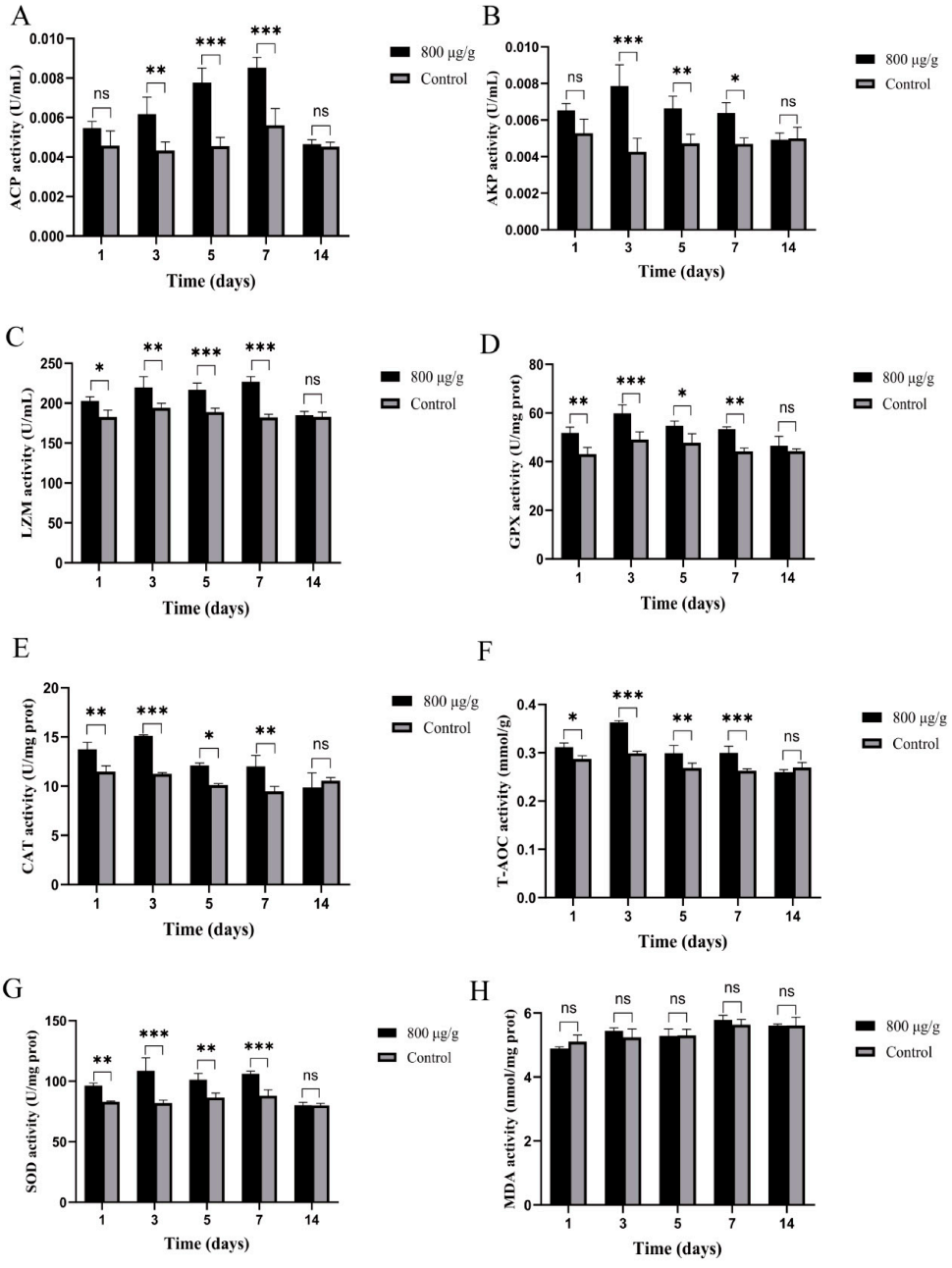

Figure 8. Effects of CPC on immune and antioxidant enzyme activities in *E. sinensis*. (**A**) Serum acid phosphatase (ACP) activity; (**B**) serum alkaline phosphatase (AKP) activity; (**C**) serum lysozyme (LZM) activity; (**D**) hepatopancreatic glutathione peroxidase (GPX) activity; (**E**) hepatopancreatic catalase (CAT) activity; (**F**) hepatopancreatic total antioxidant capacity (T-AOC); (**G**) hepatopancreatic superoxide dismutase (SOD) activity; (**H**) hepatopancreatic malondialdehyde (MDA) content. Data are presented as mean ± standard error of the mean (SEM). The number of asterisks indicates different significant differences (* < 0.05, ** < 0.01, *** < 0.001; ns, not significant).

In the hepatopancreas, the activities of antioxidant enzymes, including catalase (CAT), superoxide dismutase (SOD), and glutathione peroxidase (GPX), were significantly elevated in the CPC-supplemented group. Meanwhile, the malondialdehyde (MDA) content did not show a significant increase, suggesting that CPC enhanced the antioxidant capacity without inducing notable lipid peroxidation or oxidative damage at the tested concentration.

Collectively, these results indicated that dietary CPC at 800 μg/g could transiently enhance the non-specific immunity and antioxidant defense of *E. sinensis* during the administration period without causing obvious oxidative stress [9,23].

3.4. In Vivo Efficacy and Safety Evaluation

A 4-week high-dose safety trial was conducted to evaluate the potential lethal toxicity of CPC. During this trial, the cumulative mortality rates in the CPC-treated group and the control group were 8.3% and 6.7%, respectively, with no significant difference between the two groups (Figure 9), indicating that CPC did not cause significant lethal toxicity under the tested conditions.

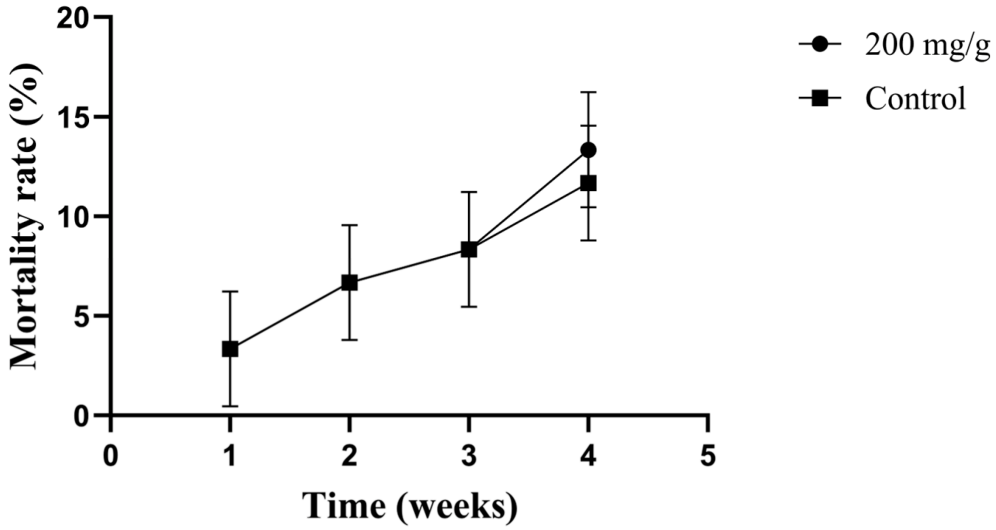

Figure 9. High-dose safety verification test of CPC on Chinese mud crabs (ecological tank $n = 3$).

Therapeutic efficacy against challenge infection. The protective effect of CPC against milky disease was further evaluated in the challenge treatment model. The raw cumulative mortality rate in group C (challenged + 800 μg/g CPC feed) was 59.72%, which was lower than that in group B (challenged + basal diet) at 75.00%, representing an absolute reduction of 15.28 percentage points. Concurrently, the tissue liquefaction rate decreased from 20.61% to 10.07%, and the pathogen re-isolation rate declined from 86.73% to 59.75% (Table 9; Figure 10).

Table 9. Statistical Results of the Treatment of "Milky Disease" in *E. sinensis* with Medicinal Preparations ($n = 3$ replicates) Values with different lowercase letters (a, ab, b, c) within the same column are significantly different ($p < 0.05$). Values sharing a common letter are not significantly different. For example, the label "ab" indicates no significant difference from groups marked with "a" or "b".

Group	Liquefaction Rate (%)	Separation Rate (%)	Death Rate (%)
Group B	20.61 ± 13.70 a	86.73 ± 7.09 a	75.00 ± 7.22 a
Group C	10.07 ± 11.81 ab	59.75 ± 23.67 ab	59.72 ± 6.37 ab
Group A	0.00 ± 0.00 b	0.00 ± 0.00 c	22.22 ± 6.36 b

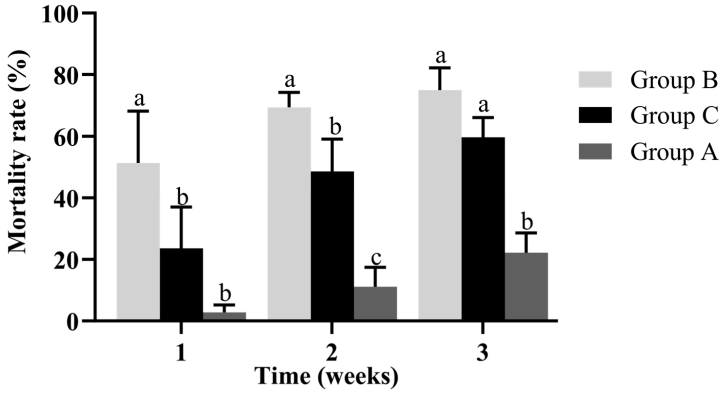

Figure 10. Statistical results of the treatment of milky disease in *E. sinensis* using bait. At the same time point, different lowercase letters (a, b, c) above the bars indicate significant differences among different groups (Group B, Group C, and Group A) ($p < 0.05$), while the same letter indicates no significant difference ($p > 0.05$).

Given that the mortality data were binomially distributed and exhibited variation among replicate rearing tanks, a generalized linear mixed model (GLMM) was applied for adjusted analysis, with the treatment group as a fixed effect, the replicate tank as a random effect, and the daily cumulative mortality counts as a covariate. After adjustment, the estimated survival rates for groups A (healthy control), C (CPC treatment), and B (challenge control) were 77.8% (95% CI: 67.9–85.3%), 40.0% (95% CI: 30.2–50.7%), and 24.4% (95% CI: 16.5–34.5%), respectively. The pairwise comparison between groups C and B yielded an odds ratio (OR) of 2.06 (95% CI: 0.92–4.63), which, after Tukey's adjustment for multiple comparisons, showed a *p*-value of 0.068 (Table 10; Figure 11). This result indicates that the survival benefit conferred by CPC administration did not reach statistical significance at the $\alpha = 0.05$ level. Nevertheless, the observed effect size (OR $\approx$ 2.06) is biologically meaningful and warrants further validation with an expanded sample size.

Table 10. Corrected survival rates and paired comparisons for each group based on generalized linear mixed model (GLMM) (ecological tanks $n = 3$ repetitions). *p*-values were corrected for multiple comparisons using the Tukey method; CI = confidence interval; OR = odds ratio (with the leftmost group in the row as the reference).

Treatment Group	Corrected Survival Rate (%), 95% CI	Pairwise Comparison	Ratio (OR)	95% CI	*p*-Value
Group A	77.8 (67.9–85.3)	To Group B	10.86	5.59–21.10	<0.0001
Group B	24.4 (16.5–34.5)	To Group C	2.06	0.92–4.63	0.068
Group C	40.0 (30.2–50.7)	To Group A	0.19	0.10–0.37	<0.0001

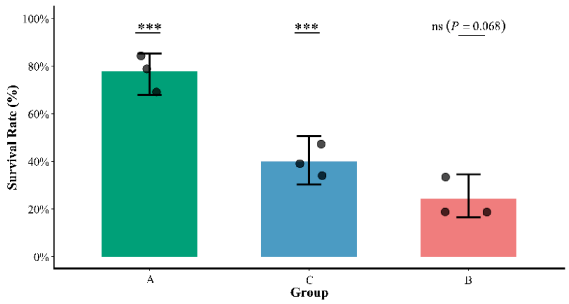

Figure 11. GLMM-corrected results for survival rates of different treatment groups. The corrected survival rates of each treatment group (least squares mean and its 95% confidence interval) and the original data of each replicate ($n = 3$ replicates). (*** < 0.001; ns, not significant).

In summary, CPC exhibited a favorable safety profile under the experimental conditions, significantly reduced tissue pathological damage, and showed a trend toward improved survival, although the statistical power was insufficient to confirm a definitive survival benefit.

3.5. Histopathological Results

To quantitatively assess the histopathological damage and verify the protective effect of CPC, a semi-quantitative scoring system was adopted, with scores ranging from zero (normal) to three (severe lesion). Double-blind evaluation was performed by two independent observers blinded to the treatment groups, who randomly selected five microscopic fields per tissue per crab. Group comparisons were conducted using the non-parametric Mann–Whitney *U* test. As summarized in Table 11, the pathological scores for the hepatopancreas, gills, muscles, and heart in group C (challenge + CPC) were significantly lower than those in group B (challenge alone) (all $p < 0.001$), confirming that CPC effectively alleviated multi-organ pathological damage.

Table 11. Comparison of main histopathological scores of *E. sinensis* in different groups [M (P25, P75)]. Scoring criteria—0 point = normal, 1 point = mild lesion, 2 points = moderate lesion, 3 points = severe lesion; Mann–Whitney *U* test, two-tailed; $p < 0.05$ indicates statistically significant differences. "-" indicates that no comparison was conducted between these groups.

Organs/Tissues	Group	*n*	Pathological Score [M (P25, P75)]	*p*-Value (B vs. C)
Liver Pancreas	A	8	0.0 (0.0, 0.0)	-
	B	8	2.25 (1.875, 2.5)	<0.001
	C	8	0.5 (0.5, 1.0)	
Gills	A	8	0.0 (0.0, 0.0)	-
	B	8	2.5 (1.875, 2.625)	<0.001
	C	8	0.5 (0.375, 0.625)	
Muscle	A	8	0.0 (0.0, 0.0)	-
	B	8	2.0 (1.5, 2.125)	<0.001
	C	8	0.5 (0.375, 0.625)	
Heart	A	8	0.0 (0.0, 0.0)	-
	B	8	1.5 (0.875, 2.0)	<0.001
	C	8	0.25 (0.0, 0.5)	

The hepatopancreas of healthy crabs (group A) exhibited neatly arranged hepatopancreatic tubules, distinct cellular architecture, and an intact basement membrane (Figure 12A). In the challenge control group (group B), prominent hydropic degeneration was observed in some tubules, with blurred cell boundaries, disorganized tubular arrangement, increased vacuolation, extensive basement membrane rupture, and cellular debris within the lumina (Figure 12B). In the CPC-treated group (Group C), the overall hepatopancreatic structure remained relatively intact, with only a small number of tubules showing mild lesions; the degree of basement membrane damage and vacuole formation was markedly lower than that in group B (Figure 12C).

Distinct differences were also observed in the gill tissues among the three groups (Figure 13). The gills of healthy crabs (group A) showed a clear and orderly external morphology with no foreign bodies in the hemocoel (Figure 13A). In group B, gill epithelial cells were damaged, the septa between hemocoels became indistinct, and abundant *M. bicuspidata* cells were present within the hemocoel (Figure 13B). In contrast, gill tissues from group C exhibited no obvious structural damage (Figure 13C).

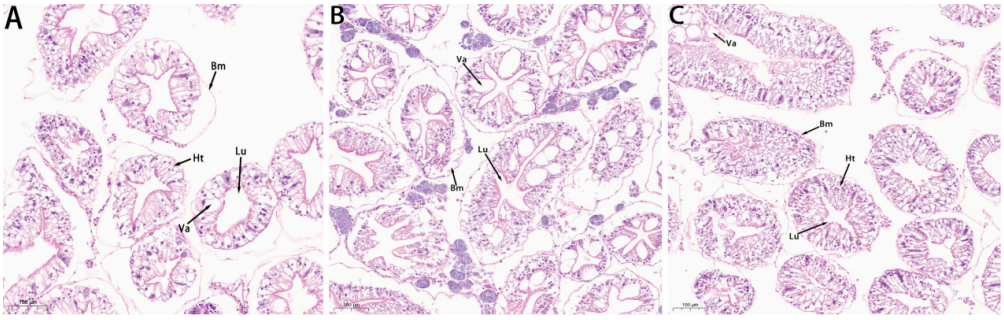

Figure 12. Pathological examination of the hepatopancreas (200 ×, *n* = 8 replicates per group). (**A**) Healthy control group; (**B**) challenge control group (infected, untreated); (**C**) challenge + CPC treatment group. Ht, hepatopancreatic tubule; Bm, basement membrane; Lu, lumen; Va, vacuole. Scale bars = 100 μm.

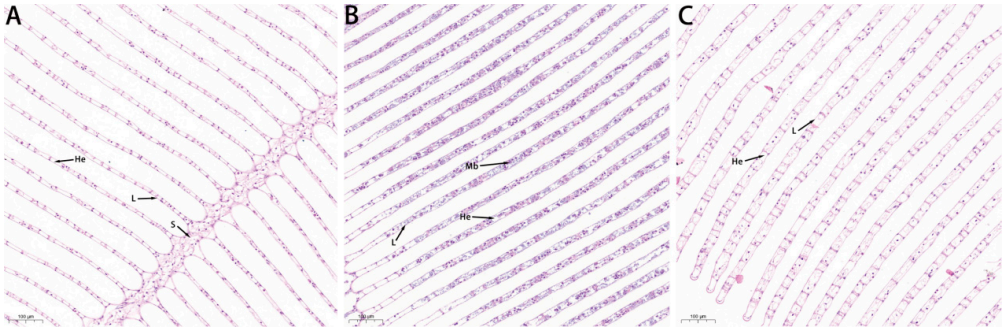

Figure 13. Pathological examination of the gills (200×, *n* = 8 replicates per group). (**A**) Healthy control group; (**B**) challenge control group (infected, untreated); (**C**) challenge + CPC treatment group. S, gill axis; L, gill lamella; He, hemocoel; Mb, *M. bicuspidata*. Scale bars = 100 μm.

Muscle tissues also showed significant intergroup differences (Figure 14). Muscle fibers in healthy crabs (Group A) were densely packed and regularly arranged (Figure 14A). In group B, muscle fibers were loosely arranged with numerous vacuoles (Figure 14B). In group C, the overall muscle structure remained intact, with only occasional vacuoles present (Figure 14C).

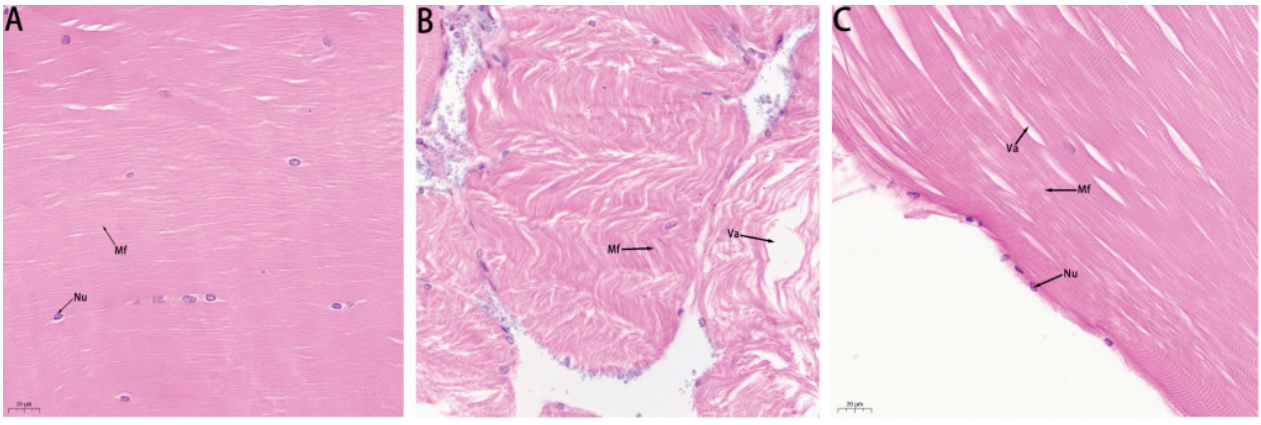

Figure 14. Pathological examination of muscle tissues (800×, *n* = 8 replicates per group). (**A**) Healthy control group; (**B**) challenge control group (infected, untreated); (**C**) challenge + CPC treatment group. Nu, nucleus; Mf, muscle fiber; Va, vacuole. Scale bars = 20 μm.

Pathological differences in the heart tissues were similarly evident among groups (Figure 15). Hearts from healthy crabs (group A) exhibited an intact structure with no

myocardial fiber rupture (Figure 15A). In group B, partial myocardial fiber rupture was observed, with abundant *M. bicuspidata* cells distributed between the fibers (Figure 15B). In group C, no foreign bodies were found between the myocardial fibers, and the tissue structure remained intact, showing marked improvement over group B (Figure 15C).

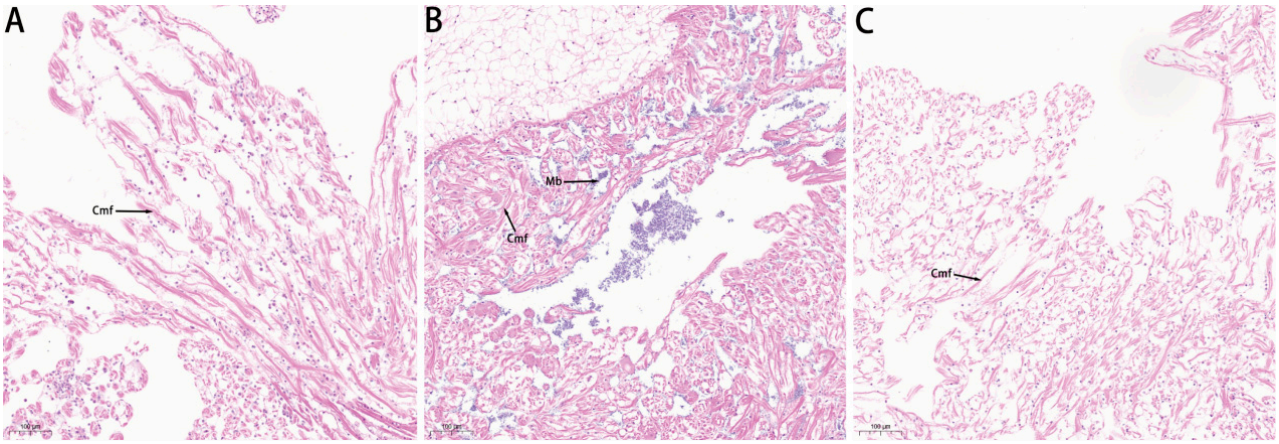

Figure 15. Pathological examination of heart tissues (200×, n = 8 replicates per group). (**A**) Healthy control group; (**B**) challenge control group (infected, untreated); (**C**) challenge + CPC treatment group. Cmf, cardiac muscle fibers; Mb, *M. bicuspidata*. Scale bars = 100 µm.

In summary, both morphological observations and semi-quantitative scoring consistently demonstrated that dietary CPC supplementation effectively alleviated the pathological damage induced by *M. bicuspidata* infection in the hepatopancreas, gills, muscles, and heart of *E. sinensis*, significantly reducing lesion severity and protecting the structural integrity of these vital organs. These results provide strong evidence for the therapeutic potential of CPC against milky disease.

4. Discussion

This study employed an integrated approach combining virtual screening, in vitro antifungal assays, and in vivo efficacy evaluation to systematically assess the potential of cetylpyridinium chloride (CPC) against milky disease in *E. sinensis*. Our results demonstrate that CPC not only exhibits significant inhibitory activity against *M. bicuspidata* but also enhances host immunity and antioxidant capacity, collectively contributing to reduced post-infection mortality and alleviating tissue damage.

4.1. Potential Molecular Mechanism: Computational Predictions and Limitations

Molecular docking revealed that CPC could bind to the predicted active site of CYP51 with a binding energy of −9 kcal/mol, with the binding site located adjacent to the heme region—a pattern similar to that of certain azole antifungals [27]. CYP51 is known to play a critical role in ergosterol biosynthesis, and its inhibition can disrupt fungal cell membrane integrity [28].

However, it must be explicitly acknowledged that the proposed targeting of CYP51 by CPC is currently based solely on computational simulation (molecular docking) and indirect inference from in vitro antifungal phenotypes. Direct experimental validation—such as CYP51 enzymatic activity inhibition assays (IC_{50} determination), sterol metabolite profiling (e.g., ergosterol content quantification via HPLC), or target gene expression analysis (e.g., ERG11 transcriptional response)—has not yet been performed. Therefore, CYP51 should be regarded as a predicted potential binding partner rather than a validated target at this stage.

On the other hand, as a quaternary ammonium compound, CPC possesses cationic surfactant properties and can directly act on microbial cell membranes, exerting broad-spectrum antifungal effects through membrane integrity disruption, permeability alteration, and cytoplasmic leakage. This non-specific membrane-damaging mechanism has been well-documented across various microorganisms. Given the collective evidence, a more plausible interpretation is that the anti-*M. bicuspidata* activity of CPC may result from a membrane-disruption-dominant mechanism [29], potentially supplemented by intracellular enzyme interference (e.g., CYP51). Such a multi-target mode of action may offer theoretical advantages in mitigating drug resistance development. However, the relative contribution of each component requires clarification through future mechanistic studies.

4.2. Antifungal Activity and Biofilm Inhibition Characteristics

In vitro assays demonstrated that CPC effectively inhibited *M. bicuspidata* at low concentrations, with MIC and MFC values at relatively low levels, indicating potent fungistatic and fungicidal activity. Additionally, CPC exhibited a marked inhibition of biofilm formation, with a discernible intervention effect observed at an early stage.

Biofilm formation is a critical strategy employed by many fungi to enhance environmental adaptability and develop drug resistance; its complex extracellular matrix can effectively impede drug penetration [30]. The ability of CPC to inhibit biofilm formation suggests that it acts not only on planktonic cells but also interferes with pathogen colonization and dissemination within the host—a property that may be particularly valuable during the early phase of infection [5].

4.3. Host Immunomodulatory and Antioxidant Effects

In addition to its direct pathogen-inhibitory effects, CPC significantly modulated the immune and antioxidant systems of *E. sinensis*. The elevated activities of immune-related enzymes—including ACP, AKP, and LZM—indicated activation of non-specific immune responses, which are crucial for eliminating invading pathogens [2].

Concurrently, the activities of antioxidant enzymes (CAT, SOD, and GPX) were markedly increased, while MDA levels did not rise significantly, suggesting that, at the tested concentration, CPC enhanced antioxidant capacity without inducing substantial oxidative damage. This regulatory profile of "enhanced defense without excessive activation" may help maintain physiological homeostasis of the pathogen [31].

Notably, immune and antioxidant indicators gradually returned to baseline levels following drug withdrawal, indicating that the regulatory effects of CPC are reversible to some extent and do not impose a persistent physiological burden—a feature with positive implications for long-term application in aquaculture.

4.4. In Vivo Protective Efficacy and Application Potential

The challenge protection experiment further validated the practical protective efficacy of CPC. Compared with the challenge control group, the CPC-treated group showed a downward trend in mortality, along with reduced rates of tissue liquefaction and pathogen re-isolation. Histopathological examination confirmed that CPC effectively alleviated pathological structural damage in key organs, including the hepatopancreas and gills.

Collectively, these findings indicate that CPC exerts not only in vitro antifungal activity but also multi-level host-protective effects in vivo. This dual-action mode—direct antifungal activity combined with host immunomodulation—confers certain advantages in aquatic disease management [32]. Furthermore, CPC is widely available, cost-effective, and has a long-standing safety record in consumer products, supporting its practical applicability in aquaculture settings.

4.5. Research Limitations and Future Directions

Despite the meaningful findings obtained, several important limitations should be carefully considered when interpreting the results.

4.5.1. Survival Benefit Did Not Reach Statistical Significance

In the challenge experiment, the CPC group exhibited an approximately 15-percentage-point higher survival rate than the control group. However, after GLMM correction, the *p*-value was 0.068. This borderline result may be attributable to (i) substantial individual variability among aquatic animals, with a sample size of 90 crabs per group potentially providing insufficient statistical power (raising the risk of type II error); (ii) the high infection load in the immersion challenge model (1×10^7 CFU/mL for 2 days), which may impose excessive physiological stress on the host and partially mask the protective effect; and (iii) inter-replicate variation, with the random effect absorbing part of the degrees of freedom [33]. Future studies should expand the sample size and consider optimizing the challenge protocol (e.g., using graded infection doses) to obtain more robust efficacy estimates [34].

4.5.2. Lack of Direct Experimental Evidence for CYP51 Targeting

As previously noted, the molecular-docking results are only preliminary. Subsequent validation—or refutation—should be pursued through enzymatic activity assays, sterol metabolic profiling, and gene expression analyses.

4.5.3. Absence of Pharmacokinetic and Food Safety Data

This study did not determine the absorption, distribution, metabolism, and elimination (ADME) profile of CPC in *E. sinensis*, nor did it assess drug residues in edible tissues—both of which are essential for evaluating the real-world application safety of CPC [8].

Additionally, no positive control drug (e.g., fluconazole) was included in the in vivo challenge experiment. Although fluconazole has demonstrated potent in vitro inhibitory activity against *M. bicuspidata*, its in vivo efficacy in *E. sinensis* remains to be systematically evaluated, and the use of such antibiotics in aquaculture is increasingly restricted due to environmental and resistance concerns [35]. Therefore, the absence of a fluconazole-treated group precludes a direct comparison of CPC's relative efficacy, and the observed effects of CPC should be interpreted with this limitation in mind.

4.5.4. Lack of a Positive Drug Control

The in vivo experiment did not include fluconazole or other established antifungal agents as reference compounds, making it difficult to benchmark the clinical or production-level significance of the observed CPC effects [34].

4.5.5. Biofilm Inhibition Concentration Setting

The concentration used for efficient biofilm inhibition (3.125 μg/mL) approached or reached the MFC. Therefore, the observed reduction in biofilm mass may be partially attributable to the killing of planktonic cells rather than specific interference with biofilm formation processes per se. Future mechanistic studies should be conducted at sub-inhibitory concentrations (e.g., 1/2 MIC) to differentiate these effects [36].

Future directions should include (i) integrating transcriptomic or metabolomic approaches for a system-level analysis of the action network; (ii) optimizing dosing strategies (e.g., sustained-release formulations, pulsed administration) to improve bioavailability; and (iii) evaluating ecological safety and long-term application effects under larger-scale simulated aquaculture conditions.

5. Conclusions

This study shows that cetylpyridinium chloride (CPC) has significant in vitro antifungal activity against *M. bicuspidata* and can effectively reduce biofilm formation under test conditions. In the in vivo experiments, CPC can significantly increase the antioxidant enzyme activity and non-specific immune indicators of *E. sinensis*, significantly alleviating tissue pathological damage in the liver, pancreas, gills, muscles, and heart, and no obvious toxicity was observed at the given dosage in this experiment. In the challenge test, the survival rate of the CPC group showed an improvement trend, but after statistical correction, it did not reach a significant level (p = 0.068), suggesting that its protective efficacy needs further verification with a larger sample. Molecular-docking studies suggest that CYP51 is a potential binding target of CPC, but its role as a direct action target still requires direct evidence from enzymology and metabolic levels. In summary, CPC, as a candidate compound for drug repurposing, shows certain application potential in the green control of milky disease in *E. sinensis*. However, its mechanism of action, pharmacokinetic characteristics and ecological safety need to be further clarified before providing sufficient evidence for its standardized application in aquaculture.

Author Contributions: All authors contributed to the study conception and design. All authors contributed to the conception and design of the study. F.Z. and C.Z. (Chunyu Zhu) conceptualized the study. X.W. drafted the original manuscript. Y.Z. and C.Z. (Changbo Zhou) performed experiments, prepared materials, collected and analyzed data. J.W. validated the data. F.Z. acquired funding and managed the project. All authors have read and agreed to the published version of the manuscript.

Funding: This work was supported by the Joint Program of Science and Technology Plan of Liaoning Province (Grant No. 2024012070-JH4/4800). This work was supported by the Natural Science Foundation of Liaoning Province (Grant No. 2024-MS-003).

Institutional Review Board Statement: This research was done under ethical and experimental animal committees of Liaoning University (approval number: 202409010; approval date: 10 September 2024).

Informed Consent Statement: Not applicable.

Data Availability Statement: The data that support the findings of this study are available from the corresponding author upon reasonable request.

Conflicts of Interest: The authors declare no conflict of interest.

References

1. Chen, D.-W.; Zhang, M.; Shrestha, S. Compositional characteristics and nutritional quality of Chinese mitten crab (*Eriocheir sinensis*). *Food Chem.* **2007**, *103*, 1343–1349. [CrossRef]
2. Hao, S.; Luo, Z.; Bai, X.; You, H.; Liu, X.; Liu, H.; Jiang, H.; Xu, X. Effects of pathogenic yeast *Metschnikowia bicuspidata* infection on immune function and intestinal microflora of the Chinese mitten crab *Eriocheir sinensis*. *Aquaculture* **2025**, *608*, 742706. [CrossRef]
3. Jiang, H.; Bao, J.; Xing, Y.; Li, X.; Chen, Q. Comparative Genomic Analyses Provide Insight into the Pathogenicity of *Metschnikowia bicuspidata* LNES0119. *Front. Microbiol.* **2022**, *13*, 939141. [CrossRef] [PubMed]
4. Hansali, K.; Zhang, Z.-R.; Liu, G.-L.; Chi, Z.; Chi, Z.-M. The Pathogenic Yeast *Metschnikowia bicuspidata* var. *bicuspidata* in the Aquacultured Ecosystem and Its Biocontrol. *J. Fungi* **2023**, *9*, 1024. [CrossRef] [PubMed]
5. Pu, S.; Chen, Z.; Sheng, D.; Shan, Y.; Zhou, P.; Shi, X.; Hao, K.; Ye, S. Screening and identification of *Aspergillus sclerotiorum* with activity against *Metschnikowia bicuspidata* and initial application on "milky disease" in *Eriocheir sinensis*. *Aquaculture* **2025**, *595*, 741653. [CrossRef]
6. Jiang, H.; Bao, J.; Xing, Y.; Cao, G.; Li, X.; Chen, Q. Metabolomic and metagenomic analyses of the Chinese mitten crab *Eriocheir sinensis* after challenge with *Metschnikowia bicuspidata*. *Front. Microbiol.* **2022**, *13*, 990737. [CrossRef] [PubMed]
7. Ma, H.; Lu, X.; Liu, J.; Guo, S.; Zhao, X.; Ye, S. *Metschnikowia bicuspidata* isolated from milky diseased *Eriocheir sinensis*: Phenotypic and genetic characterization, antifungal susceptibility and challenge models. *J. Fish Dis.* **2021**, *45*, 41–49. [CrossRef] [PubMed]

8. Fang, L.; Huang, Z.; Fan, L.; Hu, G.; Qiu, L.; Song, C.; Chen, J. Health risks associated with sulfonamide and quinolone residues in cultured Chinese mitten crab (*Eriocheir sinensis*) in China. *Mar. Pollut. Bull.* **2021**, *165*, 112184. [CrossRef] [PubMed]
9. Liu, J.; Yu, J.; Pu, S.; Shi, X.; Li, Y.; Zhao, X.; Ye, S. The complete mitochondrial genome sequence of the *Metschnikowia bicuspidata* (Metschnikoff, 1884), an emerging pathogen of 'milky disease' in Chinese mitten crab. *Mitochondrial DNA Part B* **2022**, *7*, 1277–1279. [CrossRef] [PubMed]
10. Song, J.; Zhang, S.; Lu, L. Fungal cytochrome P450 protein Cyp51: What we can learn from its evolution, regulons and Cyp51-based azole resistance. *Fungal Biol. Rev.* **2018**, *32*, 131–142. [CrossRef]
11. Zhang, R.; Wang, Y.; Wu, A.; Wang, J.; Zhang, J. Strategies of targeting CYP51 for IFIs therapy: Emerging prospects, opportunities and challenges. *Eur. J. Med. Chem.* **2023**, *259*, 115658. [CrossRef] [PubMed]
12. Tjahjono, D.H.; Chua, H.M.; Moshawih, S.; Kifli, N.; Goh, H.P.; Ming, L.C. Insights into the computer-aided drug design and discovery based on anthraquinone scaffold for cancer treatment: A systematic review. *PLoS ONE* **2024**, *19*, e0301396. [CrossRef] [PubMed]
13. Fadlalla, M.; Ahmed, M.; Ali, M.; Elshiekh, A.A.; Yousef, B.A. Molecular Docking as a Potential Approach in Repurposing Drugs Against COVID-19: A Systematic Review and Novel Pharmacophore Models. *Curr. Pharmacol. Rep.* **2022**, *8*, 212–226. [CrossRef] [PubMed]
14. Araujo, H.C.; Arias, L.S.; Caldeirão, A.C.M.; Assumpção, L.C.D.F.; Morceli, M.G.; de Souza Neto, F.N.; de Camargo, E.R.; Oliveira, S.H.P.; Pessan, J.P.; Monteiro, D.R. Novel Colloidal Nanocarrier of Cetylpyridinium Chloride: Antifungal Activities on Candida Species and Cytotoxic Potential on Murine Fibroblasts. *J. Fungi* **2020**, *6*, 218. [CrossRef] [PubMed]
15. Riveira-Muñoz, E.; Garcia-Vidal, E.; Bañó-Polo, M.; León, R.; Blanc, V.; Clotet, B.; Ballana, E. Cetylpyridinium Chloride-Containing Mouthwashes Show Virucidal Activity against Herpes Simplex Virus Type 1. *Viruses* **2023**, *15*, 1433. [CrossRef] [PubMed]
16. Zhu, X.; Li, Y.; Zhang, X.; Zhang, P.; Tian, Q.; Ma, C.; Shi, C. Combination of Cetylpyridinium Chloride and Chlorhexidine Acetate: A Promising Candidate for Rapid Killing of Gram-Positive/Gram-Negative Bacteria and Fungi. *Curr. Microbiol.* **2023**, *80*, 97. [CrossRef] [PubMed]
17. Odhar, H.A. Molecular docking and dynamics simulation of FDA approved drugs with the main protease from 2019 novel coronavirus. *Bioinformation* **2020**, *16*, 236–244. [CrossRef] [PubMed]
18. Braga, P.C.; Culici, M.; Alfieri, M.; Dal Sasso, M. Thymol inhibits *Candida albicans* biofilm formation and mature biofilm. *Int. J. Antimicrob. Agents* **2008**, *31*, 472–477. [CrossRef] [PubMed]
19. Chen, X.; Lu, X.; Wu, F.; Ge, Y.; Wang, C.; Sun, Y.; Cheng, Y. Effects of dietary supplementation with distiller grain fermented liquid on growth performance, digestive and antioxidant capacity, and intestinal microbiota in juvenile Chinese mitten crab (*Eriocheir sinensis*). *Aquac. Rep.* **2026**, *47*, 103441. [CrossRef]
20. Webb, L.; Manzi, F.; Wolinska, J. Size Matters: The Effects of Polystyrene Nanoplastics on Parasite Transmission in the Daphnia-Metschnikowia Host–Parasite System. *Freshw. Biol.* **2024**, *70*, e14359. [CrossRef]
21. Yu, Y.; You, S.; Feng, C.; Li, X.; Xing, Y.; Hu, Q.; Bao, J.; Jiang, H. First report of *Metschnikowia bicuspidata* infection in the oriental river prawn (*Macrobrachium nipponense*, de Haan) in China. *J. Fish Dis.* **2024**, *48*, e13936. [CrossRef] [PubMed]
22. Wang, Y.; Feng, C.; Xing, Y.; Hu, Q.; Li, X.; Bao, J.; Jiang, H. Morphological transformation and pathogenicity of *Metschnikowia bicuspidata* in Chinese mitten crab (*Eriocheir sinensis*). *Aquaculture* **2025**, *597*, 741921. [CrossRef]
23. Bao, J.; Jiang, H.; Shen, H.; Xing, Y.; Feng, C.; Li, X.; Chen, Q. First description of milky disease in the Chinese mitten crab *Eriocheir sinensis* caused by the yeast *Metschnikowia bicuspidata*. *Aquaculture* **2021**, *532*, 735984. [CrossRef]
24. Shi, X.; Sun, N.; Liu, J.; Pu, S.; Chen, Z.; Sheng, D.; Hao, K.; Li, X.; Ye, S. Dynamic pathology and pathogen distribution of the yeast *Metschnikowia bicuspidata* in the Chinese mitten crab (*Eriocheir sinensis*). *J. Fish Dis.* **2024**, *47*, e13993. [CrossRef] [PubMed]
25. Yu, T.; Li, Y.; Wang, W.; Lian, X.; Cheng, J.; Zuo, J.; Wang, L.; Song, L. Treatment with inactivated *Metschnikowia bicuspidata* protects against the later infection in Chinese mitten crab *Eriocheir sinensis*. *Fish Shellfish Immunol.* **2025**, *163*, 110421. [CrossRef] [PubMed]
26. Torres, P.H.M.; Sodero, A.C.R.; Jofily, P.; Silva, F.P., Jr. Key Topics in Molecular Docking for Drug Design. *Int. J. Mol. Sci.* **2019**, *20*, 4574. [CrossRef] [PubMed]
27. Warrilow, A.G.S.; Hull, C.M.; Rolley, N.J.; Parker, J.E.; Nes, W.D.; Smith, S.N.; Kelly, D.E.; Kelly, S.L.; Brakhage, A.A. Clotrimazole as a Potent Agent for Treating the Oomycete Fish Pathogen Saprolegnia parasitica through Inhibition of Sterol 14α-Demethylase (CYP51). *Appl. Environ. Microbiol.* **2014**, *80*, 6154–6166. [CrossRef] [PubMed]
28. Elsaman, H.; Golubtsov, E.; Brazil, S.; Ng, N.; Klugherz, I.; Martin, R.; Dichtl, K.; Müller, C.; Wagener, J. Toxic eburicol accumulation drives the antifungal activity of azoles against Aspergillus fumigatus. *Nat. Commun.* **2024**, *15*, 6312. [CrossRef] [PubMed]
29. Zhang, H.-Q.; Chi, Z.; Liu, G.-L.; Zhang, M.; Hu, Z.; Chi, Z.-M. *Metschnikowia bicuspidate* associated with a milky disease in *Eriocheir sinensis* and its effectitve treatment by Massoia lactone. *Microbiol. Res.* **2021**, *242*, 126641. [CrossRef] [PubMed]
30. Mohamed, E.T. Antifungal efficacy of linoleic-acid-rich Cucurbita pepo L. seed oil revealed by GC-MS profiling of lipids and bioactive markers, ergosterol depletion, and network pharmacology. *BMC Microbiol.* **2026**, *26*, 325. [CrossRef] [PubMed]

31. Shakweer, M.S.; Elshopakey, G.E.; Abdelwarith, A.A.; Younis, E.M.; Davies, S.J.; Elbahnaswy, S. Comparison of Immune Response of *Litopenaeus vannamei* Shrimp Naturally Infected with *Vibrio* Species, and after Being Fed with Florfenicol. *Fishes* **2023**, *8*, 148. [CrossRef]
32. Li, Y.; Wu, T.; Tan, X. Effects of levamisole on non-specific immune function and disease resistance of *Eriocheir sinensis*. *J. Fish. Sci. China* **2007**, *31*, 785–791.
33. Thorarensen, H.; Kubiriza, G.K.; Imsland, A.K. Experimental design and statistical analyses of fish growth studies. *Aquaculture* **2015**, *448*, 483–490. [CrossRef]
34. Mahboub, H.H.; Tartor, Y.H. Carvacrol essential oil stimulates growth performance, immune response, and tolerance of Nile tilapia to *Cryptococcus uniguttulatus* infection. *Dis. Aquat. Org.* **2020**, *141*, 1–14. [CrossRef] [PubMed]
35. Ma, H.; Sun, N.; Lu, X.; Liu, J.; Guo, S.; Zhao, X.; Ye, S. Isolation and identification of pathogen in milky disease of Chinese mitten crab *Eriocheir sinensis* in Liaoning Province. *J. Dalian Ocean Univ.* **2020**, *35*, 714–718. [CrossRef]
36. Korem, M.; Kagan, S.; Polacheck, I. The Effect of Novel Heterocyclic Compounds on Cryptococcal Biofilm. *J. Fungi* **2017**, *3*, 42. [CrossRef] [PubMed]